Pharm Res (2012) 29:3443–3454
DOI 10.1007/s11095-012-0839-9

RESEARCH PAPER

Hyaluronic Acid Derivative-Based Self-Assembled Nanoparticles for the Treatment of Melanoma

Yu-Jin Jin • Ubonvan Termsarasab • Seung-Hak Ko • Jae-Seong Shim • Saeho Chong • Suk-Jae Chung • Chang-Koo Shim • Hyun-Jong Cho • Dae-Duk Kim

Received: 28 March 2012 / Accepted: 16 July 2012 / Published online: 11 August 2012

ABSTRACT

Purpose Hyaluronic acid-ceramide (HACE)-based nanoparticles (NPs) were developed for the targeted delivery of doxorubicin (DOX), and their antitumor efficacy for melanoma was evaluated.

Methods DOX-loaded HACE-based self-assembled NPs were prepared and their physicochemical properties were characterized. The *in vitro* cytotoxicity of HACE was measured using an MTS-based assay. The cellular uptake efficiency of DOX into mouse melanoma B16F10 cells was assessed by confocal laser scanning microscopy and flow cytometry. Tumor growth and body weight were monitored after the intratumoral and intravenous injection of DOX-loaded NPs into a B16F10 tumor-bearing mouse model.

Results DOX-loaded NPs, with a mean diameter of ~110 nm, a narrow size distribution, and high drug entrapment efficiency, were prepared. A sustained DOX release pattern was shown, and drug release was enhanced at pH 5.5 compared with pH 7.4. The cytotoxicity of HACE to B16F10 cells was negligible. It was assumed that DOX was taken up into the B16F10 cells through receptor-mediated endocytosis. A significant inhibitory effect was observed on tumor growth, without any serious changes in body weight, after the injection of DOX-loaded NPs into the B16F10 tumor-bearing mouse model.

Conclusions DOX-loaded HACE-based NPs were successfully developed and their antitumor efficacy against B16F10 tumors was demonstrated.

KEY WORDS antitumor efficacy · doxorubicin · hyaluronic acid-ceramide · melanoma · nanoparticle

INTRODUCTION

Doxorubicin (DOX) is an anthraquinone anticancer drug that has been commonly used in the treatment of a wide range of cancers, including hematological malignancies, many types of carcinoma, and soft tissue sarcomas (1,2). DOX can, however, cause severe cardiotoxicity, especially heart arrhythmias (3). Therefore, tumor-targeted delivery is required for it to have an efficient anticancer effect.

Nanotechnology is frequently used for the development of various drug delivery systems (4,5). Among the various types of nano-sized drug delivery systems, self-assembled polymeric nanoparticles (NPs) have been investigated for their potential to deliver poorly water-soluble drugs, which can be incorporated into the NP's hydrophobic core (6,7). It has been reported that

Electronic supplementary material The online version of this article (doi:10.1007/s11095-012-0839-9) contains supplementary material, which is available to authorized users.

Y.-J. Jin • U. Termsarasab • S. Chong • S.-J. Chung • C.-K. Shim • D.-D. Kim (✉)
College of Pharmacy
Research Institute of Pharmaceutical Sciences
Seoul National University
Seoul 151-742, Republic of Korea
e-mail: ddkim@snu.ac.kr

S.-H. Ko • J.-S. Shim
Biogenics Inc.
Daejeon 305-510, Republic of Korea

J.-S. Shim
Skin & Tech Inc.
Seongnam 461-713, Republic of Korea

H.-J. Cho (✉)
College of Pharmacy, Sunchon National University
Suncheon 540-950, Republic of Korea
e-mail: chohj@sunchon.ac.kr

NPs with an adequate particle size (<200 nm mean diameter) and surface properties can circulate in the bloodstream for a long time and passively accumulate into the tumor region due to the enhanced permeability and retention (EPR) effect (8,9). Moreover, it is known that the hydrophilic surface of NPs can reduce the opsonization of DOX-loaded NPs (10). It is also thought that the cellular uptake of NPs could provide an enhanced anticancer effect (11,12). To overcome the limitations of passive targeting, diverse active targeting strategies have been adopted, in which the targeting moieties are attached to the surface of drug carriers (5,13).

Hyaluronic acid (HA) is a biodegradable, biocompatible, and viscoelastic linear polysaccharide, and thus has been widely investigated in terms of its potential use as a drug carrier. It is composed of alternating disaccharide units of D-glucuronic acid and *N*-acetyl-D-glucosamine with (1→4) interglycosidic linkages (14). HA is distributed throughout the extracellular matrix, connective tissues, and organs of all higher animals (15). Incorporated drugs can be sustainably released from HA-based carriers through the enzymatic hydrolysis of HA by hyaluronidase (16). HA is one of the major components of the extracellular matrix and the main ligand for the hyaluronan receptors CD44 and RHAMM, which are overexpressed in a variety of tumor types (17). Therefore, the targeting of drugs to tumors can be accomplished by receptor-mediated uptake of the drug (18,19). The ceramides (CEs) are a family of lipid molecules that are composed of sphingosine and a fatty acid. The most well-known functions of CE as a cellular signaling molecule include the regulation of the differentiation, proliferation, and apoptosis of cells (20). The tumor targetability of a hyaluronic acid-ceramide (HACE)-based NP by HA and CD44 receptor interaction was identified in a previous study by our laboratory (21).

In our previous studies (21,22), the model cancer cell lines (CD44 receptor high or low expressed cell lines) were used mainly for identifying the tumor targetability by the interaction between HA and CD44 receptors. It is necessary, however, to look into the therapeutic efficacy of the HACE-based NPs on the primary and metastatic melanoma. Thus, we herein report on the use of HACE as an amphiphilic polymer which will be used for the preparation of micellar NPs and the evaluation of the physicochemical properties of DOX-loaded HACE-based NPs. The release of DOX from the NPs and the intracellular uptake of DOX into B16F10 cells were studied. Then, the antitumor effect of DOX-loaded NPs after their intratumoral and intravenous injection was investigated in a B16F10 melanoma-bearing mouse model.

MATERIALS AND METHODS

Materials

HA oligomer (4.7 kDa) and DS-Y30 (ceramide 3B; mainly *N*-oleoyl-phytosphingosine) were purchased from Bioland Co., Ltd. (Cheonan, Korea) and Doosan Biotech Co., Ltd. (Yongin, Korea), respectively. Tetra-*n*-butylammonium hydroxide (TBA), *N*-(3-dimethylaminopropyl)-*N*′-ethylcarbodiimide (EDC), adipic acid dihydrazide (ADH), and 1-hydroxybenzotriazole (HOBt) were obtained from Sigma-Aldrich Co. (St. Louis, MO, USA). Doxorubicin hydrochloride (DOX HCl) was purchased from Boryung Pharmaceutical Co., Ltd. (Seoul, Korea). Dulbecco's modified Eagle's medium (DMEM), penicillin, streptomycin, and fetal bovine serum (FBS) were obtained from Gibco Life Technologies Inc. (Grand Island, NY, USA). All other reagents were of analytical grade and obtained from commercial sources.

Synthesis of HACE

HACE was synthesized as reported in our previous study (21). Briefly, HA (12.21 mmol) and TBA (9.77 mmol) were solubilized in 60 ml of double distilled water (DDW) and stirred for 30 min. Activated HA-TBA was acquired by lyophilization. To prepare the DS-Y30 linker, DS-Y30 ceramide (8.59 mmol) and triethylamine (9.45 mmol) in 25 ml of tetrahydrofuran (THF), and 4-chloromethylbenzoyl chloride (8.59 mmol) in 10 ml of THF were blended. The DS-Y30-containing linker was acquired by concentration and recrystallization after stirring for 6 h at 60°C. HA-TBA (8.10 mmol) and the DS-Y30-containing linker (0.41 mmol) were then dissolved in a mixture of THF and acetonitrile (4:1, *v*/*v*) and stirred for 5 h at 40°C. HACE was obtained by eliminating the impurities and organic solvent.

Preparation of DOX-Loaded HACE Nanoparticles

The methods for the preparation of the DOX base and DOX-loaded NPs were based on our previous report (22). To prepare the DOX base, 100 mg of DOX HCl was dissolved in 10 ml of anhydrous dimethyl sulfoxide (DMSO) and 0.12 ml of triethylamine was added. After 12 h of stirring at room temperature, the solution was freeze-dried and desiccated. To prepare the DOX-loaded NPs, 1 mg of DOX was dissolved in 1 ml of a mixture of DMSO and DDW (1:1, *v*/*v*). Subsequently, 6, 9, and 12 mg (for F1, F2, and F3, respectively) of HACE were added to the mixture and it was vortexed for 10 min. The solvent was evaporated under a stream

of nitrogen gas at 70°C for 4 h. To prepare the self-assembled NPs, 1 ml of DDW was added to polymer- and drug film-coated tubes and vortexed for 2 min. All samples were filtered through a syringe filter with a pore size of 0.2 μm (Minisart RC 15; Satorius Stedim Biotech GmbH, Göttingen, Germany) to remove the insoluble drug.

Characterization of DOX-Loaded HACE Nanoparticles

The mean diameter, polydispersity index and zeta potential values of the drug-loaded NPs were measured using a light-scattering spectrophotometer (ELS-Z; Otsuka Electronics, Tokyo, Japan) as described previously (22). To measure the drug encapsulation efficiency (EE), DOX-loaded NPs were disrupted with 100× the volume of DMSO, and the drug content was analyzed by high performance liquid chromatography (HPLC). As described previously (22), DOX was quantitatively analyzed with a Waters HPLC system (Waters Co., Milford, MA, USA) equipped with a reversed-phase C-18 column (Xbridge®, RP-18, 250×4.6 mm, 5 μm; Waters Co.), a separation module (Waters e2695), and a fluorescence detector (Waters 2475). The mobile phase consisted of 0.1 M sodium acetate buffer (pH 4.0 adjusted with acetic acid) and acetonitrile (71:29, *v/v*), and the eluent was monitored at excitation and emission wavelengths of 470 and 565 nm, respectively, with a flow rate of 1.0 ml/min. The injection volume for the drug analysis was 20 μl. The lower limit of quantification (LOQ) was 50 ng/ml. Acceptable precision (<4%) and accuracy (−7.23% to 4.64%) were also acquired in standard curve range (0.1–25.0 μg/ml).

The drug content and EE were calculated using the following formulas:

$$\text{Drug content}\,(\%) = \frac{\text{actual amount of DOX in NPs}}{\text{amount of NPs}} \times 100 \quad (1)$$

$$\text{EE}\,(\%) = \frac{\text{actual amount of DOX in NPs}}{\text{theoretical amount of DOX in NPs}} \times 100 \quad (2)$$

Three separately prepared NPs were used to determine the drug content (%) and EE (%), which were expressed as the mean ± standard deviation (SD).

The morphological shapes of the DOX-loaded NPs were observed without staining, using a transmission electron microscope (TEM, JEM1010; JEOL, Tokyo, Japan) operated at an acceleration voltage of 100 kV. The sample was loaded onto a copper grid, incubated for 2 min, washed with DDW, and then air-dried.

In Vitro Release Study

The *in vitro* release test was conducted in phosphate buffered saline (PBS, pH 5.5 and 7.4 adjusted with phosphoric acid) for 8 days at 37°C with a rotation speed of 50 rpm. An aliquot of each sample (150 μl) was loaded into a Mini GeBA-flex tube (molecular weight cutoff: 12–14 kDa; Gene Bio-Application Ltd., Kfar Hanagide, Israel) and then it was transferred into 10 ml of PBS (pH 5.5 and 7.4). The sampling times were 1, 2, 3, 4, 6, 9, and 12 h for DOX HCl solution group, and 1, 2, 3, 4, 6, 9, 12, 24, 48, 72, 96, 120, 144, 168, and 192 h for DOX-loaded NP group, respectively. An aliquot (0.2 ml) was collected at each sampling time, which was replaced with an equivalent volume of fresh medium. The concentration of DOX in the samples was analyzed using a previously described HPLC method.

In Vitro Cytotoxicity Test

B16F10 cells were purchased from the Korean Cell Line Bank (KCLB, Seoul, Korea). The cells were cultured with DMEM supplemented with 10% FBS, 100 U/ml penicillin, and 100 μg/ml streptomycin in a 5% CO_2 atmosphere and 95% relative humidity at 37°C. The cytotoxicity of HACE toward the B16F10 cells was evaluated using an MTS-based assay. After the B16F10 cells achieved 70–80% confluency, the cells were trypsinized and seeded onto 96-well plates at a density of 1.0×10^4 cells per well. After 24 h of incubation, the cell culture medium was eliminated. Cytotoxicity was measured after 24 and 48 h of incubation with various concentrations of HACE (0–1000 μg/ml), without drug loading, at 37°C under a 5% CO_2 atmosphere and 95% relative humidity. After the incubation period, the cells were treated with the MTS-based CellTiter 96® AQ_{ueous} One Solution Cell Proliferation Assay Reagent (Promega Corp., WI, USA) at 37°C for 4 h according to the manufacturer's protocol. The absorbance was read at a wavelength of 490 nm with an EMax Precision Microplate Reader (Molecular Devices, Sunnyvale, CA, USA).

In Vitro Cellular Uptake Study

The cellular uptake and distribution of DOX from the prepared NPs were observed by confocal laser scanning microscopy (CLSM). After the B16F10 cells achieved 70–80% confluency, the cells were trypsinized and seeded onto culture slides (BD Falcon, Bedford, MA, USA) at a density of 1.0×10^5 per well (surface area of 1.7 cm^2 per well, 4-chamber slides) and incubated for 24 h at 37°C. The DOX or the DOX-loaded NP (50 μg/ml of DOX) was added and incubated for 1 h at 37°C. After incubation, all reagents were removed. The cells were washed with PBS (pH 7.4) at least 3 times and fixed with 4% formaldehyde for 10 min. The liquid content was then dried completely. VECTASHIELD mounting medium

with 4′,6-diamidino-2-phenylindole (DAPI) (H-1200; Vector Laboratories Inc., Burlingame, CA, USA) was added to prevent fading and to stain the nuclei. The cells were then observed by CLSM (LSM 710; Carl-Zeiss, Thornwood, NY, USA).

The cellular uptake efficiency was also evaluated by flow cytometry. After the B16F10 cells obtained 70–80% confluency, the cells were detached and seeded onto a 6-well plate with a density of 6×10^5 cells per well and incubated overnight. The culture medium was removed and 50 μg/ml of DOX, alone or incorporated in the NPs, was added and incubated for 1 h. After incubation, all reagents were removed and cells were washed with PBS at least 3 times. After washing with PBS, cells were trypsinized and the supernatant was carefully removed. PBS containing 2% (*v*/*v*) FBS was added to the cell pellet and resuspended. The cells were analyzed using a FACSCalibur fluorescence-activated cell sorter (FACS™) equipped with CELLQuest software (Becton Dickinson Biosciences, San Jose, CA, USA).

In Vivo Antitumor Efficacy Test

Female C57BL/6 mice (5 weeks of age; Charles River) were used to prepare the tumor-bearing mouse model. Mice were maintained in a light-controlled room kept at a temperature of 22±2°C and a relative humidity of 55±5% (Animal Center for Pharmaceutical Research, College of Pharmacy, Seoul National University, Korea). The experimental protocols used in the animal studies were approved by the Animal Care and Use Committee of the College of Pharmacy, Seoul National University. The B16F10 cell suspension (1×10^6 cells in 0.1 ml) was subcutaneously injected into the backs of the mice. The tumor treatment was initiated 7 days after the injection, when the tumor reached a volume of approximately 50–100 mm^3. The tumor size was measured using vernier calipers, and the tumor volume (mm^3) was calculated as $V=0.5\times length\times width^2$ (23,24). The experimental groups were as follows: control, DOX solution, and HACE:DOX (12:1). DOX (at a dose of 5 mg/kg) was injected intratumorally or intravenously into each mouse on days 4, 7, 9, and 11. The tumor volumes and body weights of the mice were measured for 14 days. The tumors were then dissected on day 14 for histological staining. Tumors were fixed in 4% (*v*/*v*) formaldehyde for 1 day and 6 μm sections were deparaffinized and hydrated with ethanol. The chromogen diaminobenzene (DAB) was incubated for color development in the terminal deoxynucleotidyl transferase dUTP nick end labeling (TUNEL) assay for detecting DNA fragmentation resulting from apoptotic signaling cascades.

Statistical Analysis

Statistical analysis was performed using analysis of variance (ANOVA). All experiments were performed at least 3 times and the data were represented as the mean ± SD.

RESULTS AND DISCUSSION

Preparation and Characterization of DOX-Loaded HACE-Based NPs

HA has been used as a tumor-targeting moiety through its chemical conjugation to the other polymers or drugs and/or its use in the preparation of NPs for anticancer drug delivery (25,26). In this study, HA was used as a drug carrier and tumor-targeting moiety. An amphiphilic polymer (HACE), composed of HA (the hydrophilic part) and CE (the hydrophobic part), was synthesized (Fig. 1a). Both HA and CE have been reported to be intrinsic biological components, and thus could be regarded here as biocompatible substances for the development of drug delivery systems (27,28). CE was conjugated to HA oligomers to make an amphiphilic HA derivative, as reported previously (21). Activated HA-TBA was synthesized, and the CE, including the linker, was then attached. Chloromethylbenzoyl chloride, as a linker (L1), was conjugated to the CE by esterification, and then the linker-CE complex was conjugated to HA-TBA by ether bond formation. Critical aggregation concentrations (CACs) were determined through fluorescence studies with pyrene as a fluorescent probe. The fluorescent probe technique used is a very sensitive method for detecting the formation of polymeric micelles (29). The CAC for HACE, reported in our previous study, was 0.042 mg/ml (21). This value is lower than those of other amphiphilic polymers and indicated that the HACE-based NP could be stable after dilution in large volumes of body fluid.

A solvent evaporation method was used to encapsulate DOX into the hydrophobic core of the HACE-based NPs (Fig. 1b). Schematic diagram for preparing DOX-loaded HACE-based NPs is shown in Supplementary Fig. S1. This method is known to have the following advantages over the dialysis method: 1) it is a simple preparation method, 2) it has a short preparation period, and 3) it has a high drug loading efficiency (30). As shown in Table I, DOX-loaded HACE-based NPs with a narrow size distribution (polydispersity index <0.2) and a mean diameter of 100–120 nm were prepared. It is known that drug carriers with a diameter less than 200 nm can avoid uptake by the reticuloendothelial system (RES), circulate in the bloodstream for a prolonged time, and consequently accumulate in the region of the tumor efficiently (31–33). The surface charge values of the HACE-based NPs were negative (−24.34 to −27.02 mV) due to the

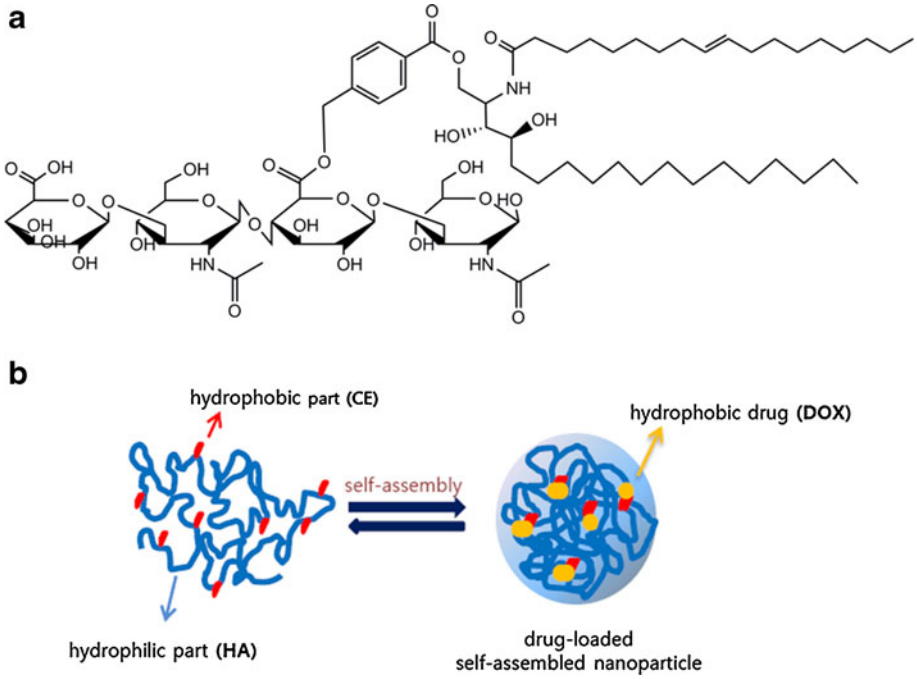

Fig. 1 The chemical structure of hyaluronic acid-ceramide (HACE) (**a**) and an illustration of the doxorubicin (DOX)-loaded HACE-based self-assembled NPs (**b**).

ionized carboxylic group of HA being located in the shell, and this implied that aggregation of the particles could be prevented by electrostatic repulsion. Considering their mean diameter, polydispersity index, and zeta potential values, it was determined that the prepared NPs could be used as efficient anticancer drug delivery systems. The morphology of the NPs was observed by TEM. As shown in Fig. 2, the NPs were observed to be round in shape and have a narrow size distribution. The influence of weight ratio between HACE and DOX on the physicochemical properties of DOX-loaded NPs was investigated. In particular, the EE of DOX in the NPs ranged from 51.20% to 73.07% (Table I), the EE of F3 being the highest. Due to its high EE, F3 was selected for the further studies.

In Vitro Drug Release Study

The *in vitro* release of DOX from DOX solution and the HACE NPs was investigated under different pH conditions (pH 7.4 and 5.5). Acidic pH condition (pH 5.5) was set up with normal physiological pH condition (pH 7.4) in this release test. The target site of DOX is cell nucleus, thereby nanoparticles have to use endocytic pathway. The cellular localization and their escape from acidic endocytic compartments (*i.e.* endosomes and lysosomes, pH 5.5) can be regarded as an important environmental condition for DOX release. Regarding carriers for DOX delivery, pH 5.5 has been also used as a representative release condition (34,35). The release of DOX from the NPs was measured for 8 days, and sustained release profiles were observed during that period (Fig. 3). Although a large amount (>70%) of DOX was released from its solution within 12 h, only 4.43±0.08% and 8.08±1.34% of DOX were released from the developed NPs at pH 7.4 and 5.5, respectively. The rapid release of DOX from the NPs in the initial period may be attributed to the DOX molecules being located on the surface of the HA shell. After 8 days, the amounts of released DOX from NPs were 17.99±1.71%

Table I The Composition and Characterization of DOX-Loaded HACE-Based NPs

Formulation	Composition	Mean diameter (nm)	Polydipersity Index	Zeta potential (mV)	Encapsulation efficiency (%)	Drug content (%)
F1	HACE:DOX (6:1)	104.28±1.97	0.19±0.02	−26.37±4.09	54.84±1.03	7.84±0.38
F2	HACE:DOX (9:1)	114.56±2.03	0.19±0.01	−27.02±2.11	51.20±4.54	5.12±0.98
F3	HACE:DOX (12:1)	109.11±0.35	0.19±0.02	−24.34±2.12	73.07±5.42	5.63±0.05

All values are presented as mean ± SD (n=3)

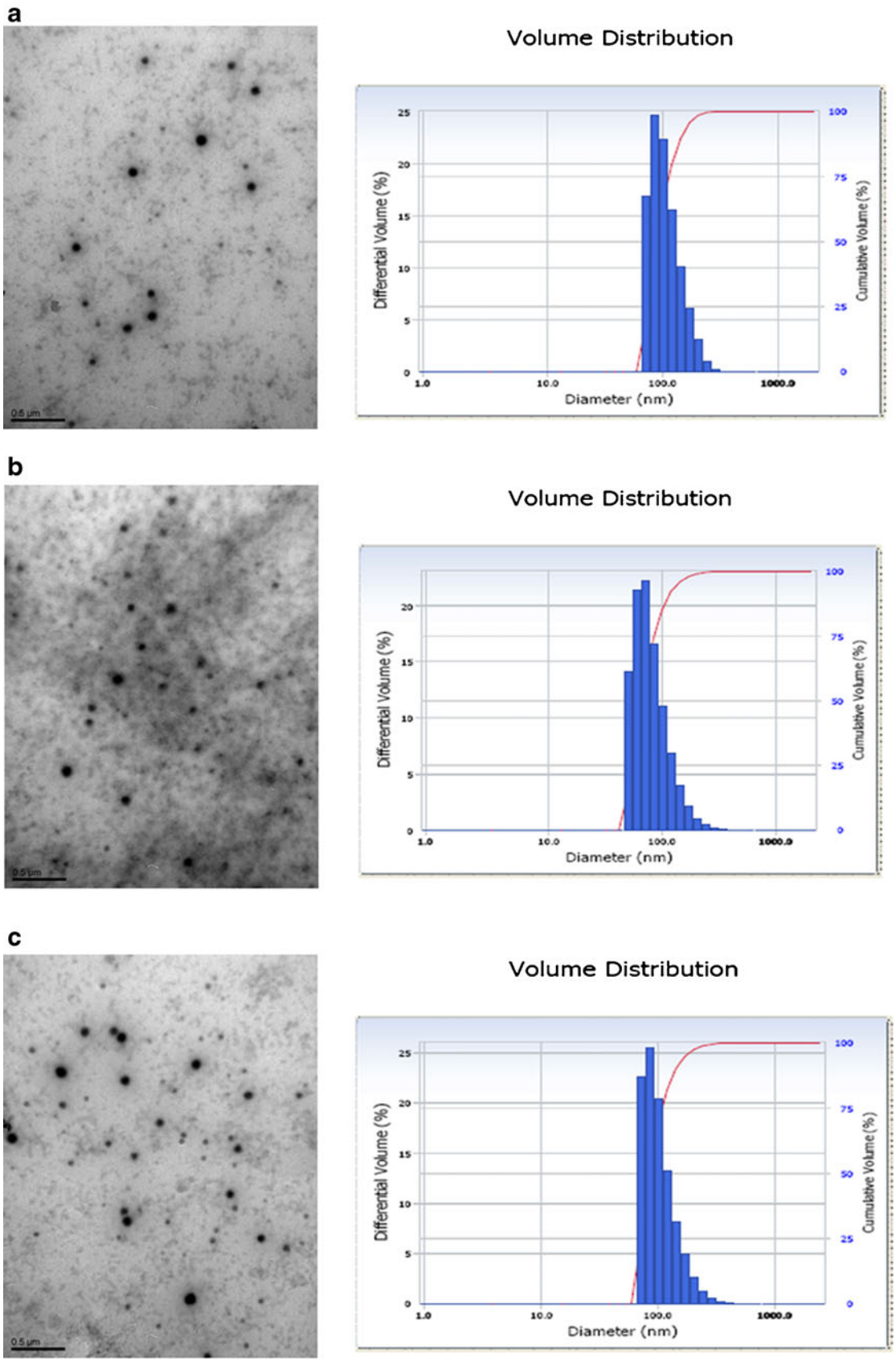

Fig. 2 Transmission electron microscopy (TEM) images (left panel) and volume distribution diagrams of the mean diameters (right panel) of (**a**) F1, (**b**) F2, and (**c**) F3. The length of the bar in the TEM image is 500 nm.

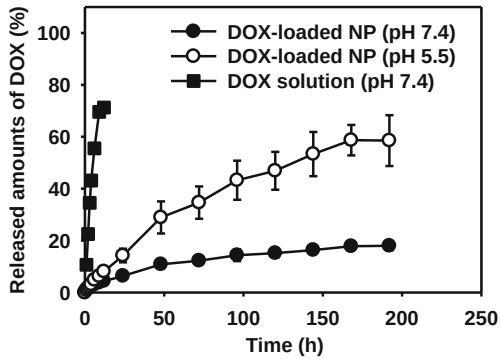

Fig. 3 *In vitro* drug release profiles of DOX solution at pH 7.4 (*black square*), and DOX-loaded NPs (HACE:DOX = 12:1, F3) at pH 5.5 (*white circle*) and 7.4 (*black circle*), respectively. Each point represents the mean ± SD (n=3).

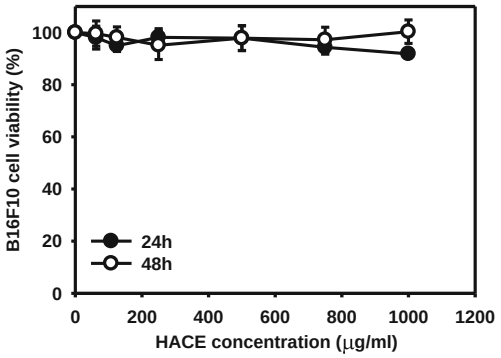

Fig. 4 *In vitro* cytotoxicity tests in B16F10 cells. The cytotoxicity of HACE at various concentrations was measured after 24 and 48 h of incubation. Cell viability (%) was measured using an MTS-based assay. The data are expressed as the mean ± SD (n=4).

and 58.53±9.80% at pH 7.4 and 5.5, respectively. Of particular note, although the release of DOX from the NPs at pH 7.4 reached a plateau after 4 days, at pH 5.5 the drug release was sustained for 7 days. The sustained release of the drug from the HACE-based NPs can be explained by a hydrophobic-hydrophobic interaction between the drug and the hydrophobic core of the HACE NPs (36,37). The sustained release of a drug can improve its *in vivo* therapeutic efficacy and thus the patient's comfort. Moreover, an enhanced DOX release profile was observed at pH 5.5 compared with at pH 7.4. It might be explained by the weakening of the binding between the nanoparticulate system and drug, and improved solubility of DOX at the acidic pH (35,38). This pH-dependent drug release pattern can play a crucial role in tumor-targeted drug delivery. It is assumed that the amount of DOX released at the physiological pH condition was relatively low. However, due to the higher release of DOX from the NP at the acidic pH (representing the conditions within endosomes/lysosomes), a higher amount of the drug could be taken up into the cell through receptor-mediated endocytosis (especially HA and CD44 receptor interaction) and reach the nucleus of the cancer cells.

In Vitro Cytotoxicity Test

The cytotoxicity of the synthesized HACE was evaluated in a mouse melanoma B16F10 cell line. The cytotoxicity was assessed at various concentrations of HACE (0–1000 μg/ml) after 24 and 48 h incubation times. CD44, one of the receptors for HA, has been reported to be expressed in B16F10 cells; thus, these cells were selected as the mouse melanoma cell line in this study (39,40). As shown in Fig. 4, the viability (%) of the B16F10 cells was >90% within the tested HACE concentration range. The *in vitro* biocompatibility of HACE in the B16F10 cells was identified in this test and it was similar to that shown for other cell lines (21,22).

In Vitro Cellular Uptake Study

The cellular uptake of DOX into the B16F10 cells was evaluated by CLSM and flow cytometry. In our previous studies (21,22), it was reported that HACE-based NPs were mainly taken up into the cells, which overexpressed the CD44 receptor, through HA and CD44 receptor interaction. Therefore, further experiments to investigate HA and CD44 receptor interaction by inhibiting the CD44 receptor were not performed in this study. As shown in Fig. 5a, the cellular uptake and distribution of DOX from the HACE-based NPs were observed by CLSM. The nuclei of the cells were stained with DAPI (blue). The fluorescence of DOX (red) from HACE-based NPs was slightly higher than that in DOX solution group. This pattern was also consistently observed in the results of the flow cytometry analysis (Fig. 5b). The values of fluorescence intensity for control, DOX solution, DOX-loaded NP groups were 3.72±0.53, 35.30±2.19, 59.04±2.26, respectively (P<0.05). It has been suggested that the cellular uptake of DOX is related to the incubation time (41). Additionally, the different patterns may be explained by differential uptake mechanisms of DOX for the two different groups, for example, passive diffusion for the DOX solution and receptor-mediated endocytosis for the DOX-loaded HACE NPs. We assumed that the DOX from the HACE NPs was successfully delivered to the nucleus, the target site of the drug, based on the overlap of red and blue staining (DAPI staining). The delivery of DOX to the nucleus can imply its consequent anticancer effect at the cellular level.

In Vivo Antitumor Efficacy Test

The *in vivo* antitumor efficacy of the developed DOX-loaded NPs was evaluated in the B16F10 tumor-bearing mouse model. The DOX-loaded NP formulation was injected

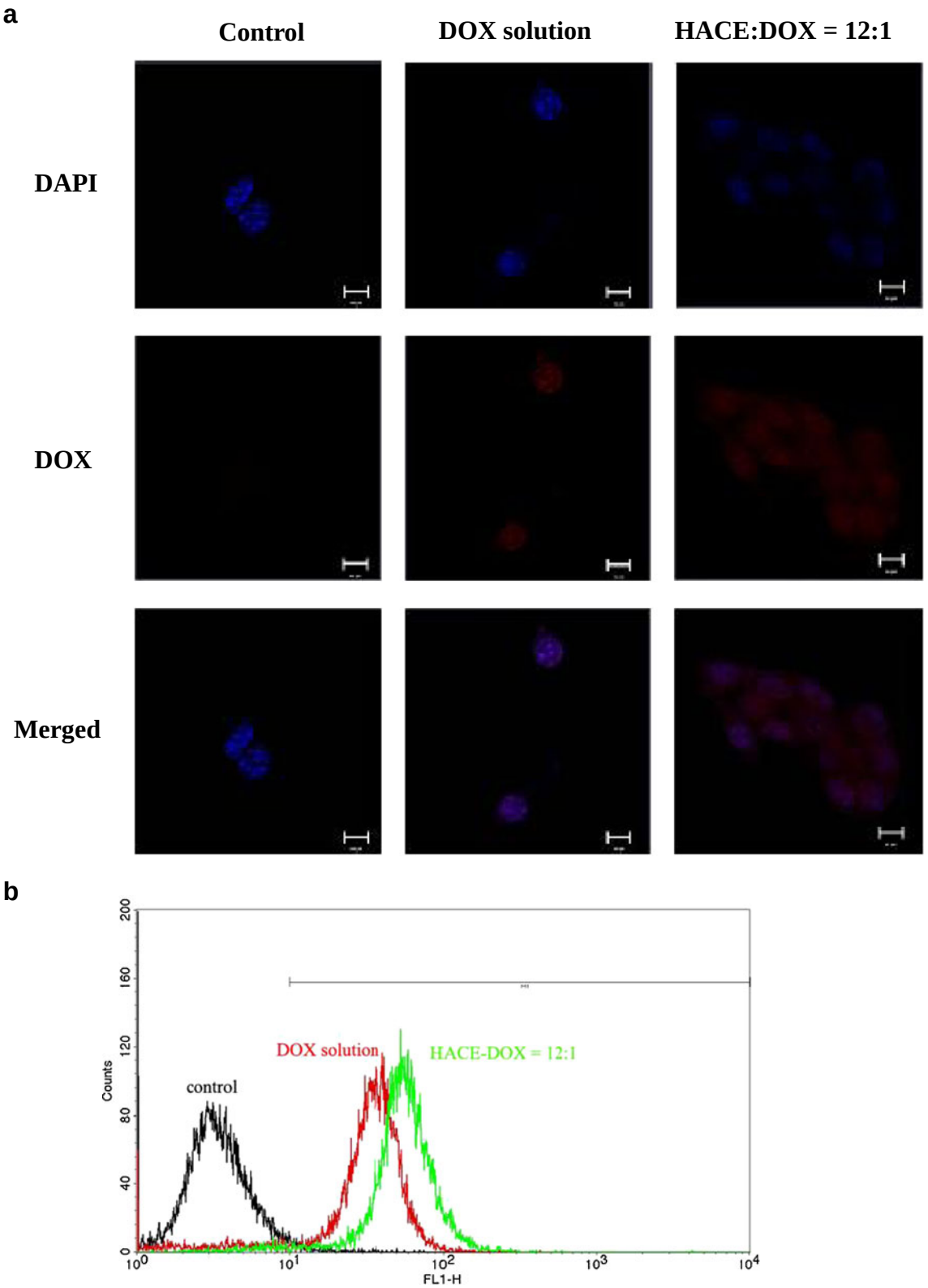

Fig. 5 *In vitro* cellular uptake study in B16F10 cells. DOX solution and DOX-loaded NPs (F3) were incubated for 1 h. (**a**) The intracellular distribution of DOX was observed by confocal laser scanning microscopy. Red and blue indicate DOX and DAPI, respectively. The length of the bar is 10 μm. (**b**) The amounts of DOX taken up into the cells were analyzed by flow cytometry (n=3). Different colors indicate different experimental groups (black: control [no treatment], red: DOX solution, green: HACE:DOX = 12:1).

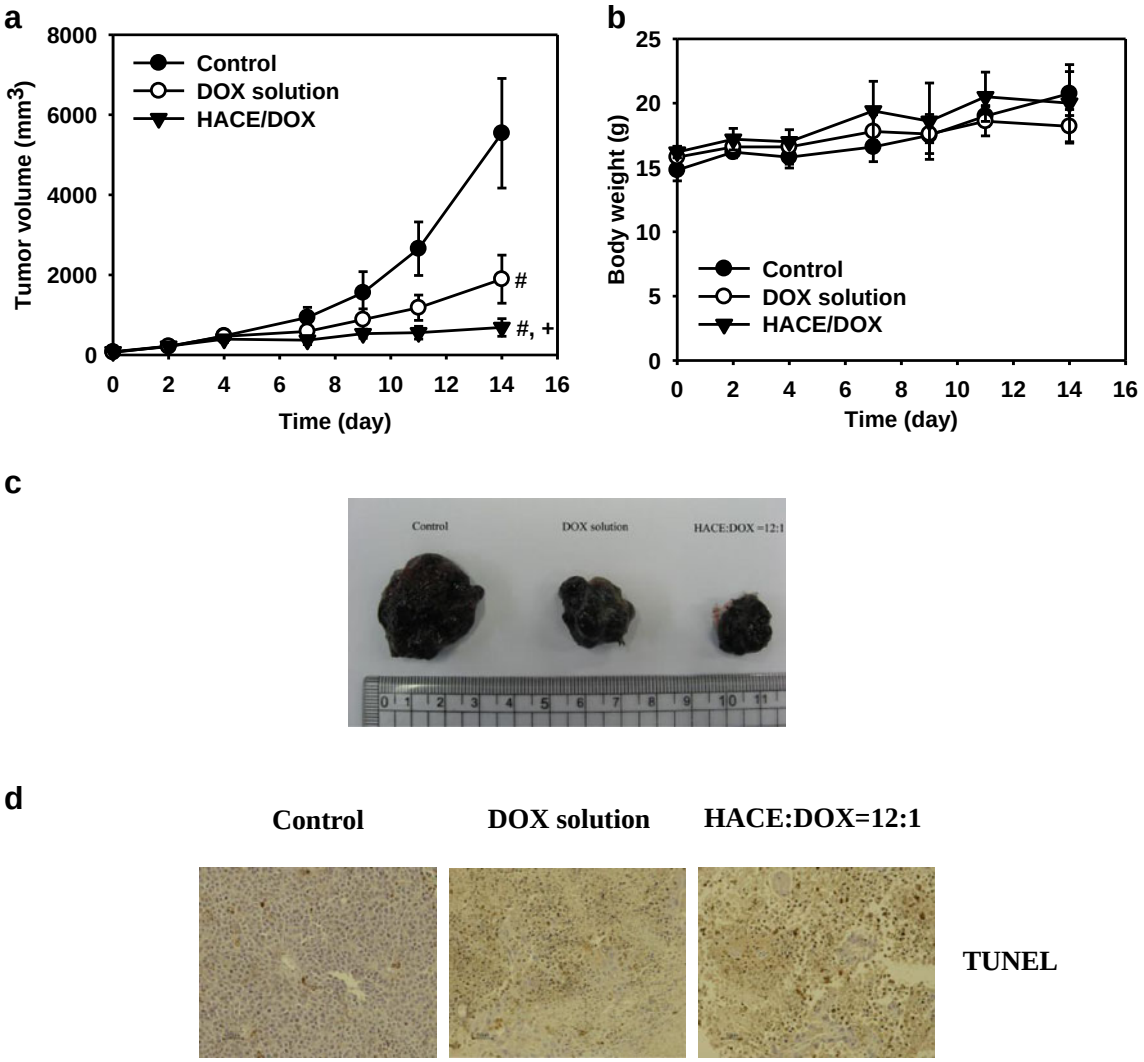

Fig. 6 *In vivo* antitumor efficacy test in the B16F10 tumor-bearing mouse model after intratumoral injection. (**a**) The tumor size (mm^3) profile. DOX was intratumorally injected at 4, 7, 9, and 11 days. $^{\#}P < 0.05$ compared with the control group; $^{+}P < 0.05$ compared with the DOX solution-treated group. (**b**) The body weight (g) profile. Each point represents the mean ± SD ($n \geq 4$). (**c**) Images of the dissected tumors of all experimental groups after 14 days. (**d**) Microscopic images of the results of the TUNEL assay of dissected tumors after 14 days. The length of the bar is 50 μm.

intratumorally and intravenously on days 4, 7, 9, and 11. The volumes of the tumors (mm^3) and the body weights of the mice (g) were monitored for 14 days, and then the tumors were dissected for TUNEL assay (Figs. 6 and 7). The growth of the tumor was significantly inhibited in the groups treated with the DOX solution and HACE/DOX compared with the control group after both the intratumoral and intravenous administrations ($P<0.05$). After the intratumoral injection, the relative tumor volumes of the DOX solution- and the DOX-loaded NP-treated groups to control group were 34.18% and 12.40% at 14 days, respectively (Fig. 6a). Following the intravenous injection, the relative tumor volumes of the DOX solution- and DOX-loaded NP-treated groups to control group were 27.09% and 10.86% at 14 days, respectively (Fig. 7a). Microscopic images of the dissected tumors on day 14 are presented in Figs. 6c and 7c. In particular, the HACE/DOX-treated group showed a stronger inhibition of tumor growth than the DOX solution-treated group irrespective of the route of injection. There was no significant difference in the body weight of the mice on day 14 between the control and HACE/DOX-treated groups, which implied that there was no serious systemic toxicity of the developed HACE-based NP formulation (Figs. 6b and 7b).

We previously demonstrated the interaction of HA and CD44, and its role in active tumor targeting (21). The suppressive effect of the HACE-based formulation on tumor growth observed in this study could be explained by both passive targeting (an EPR effect) and active targeting (an HA and CD44 receptor interaction), especially in the intravenous injection group. Besides the tumor targetability of the HACE-based NPs, it is assumed that the *in vivo* clearance of DOX after its encapsulation in the NPs can be decreased as reported in the

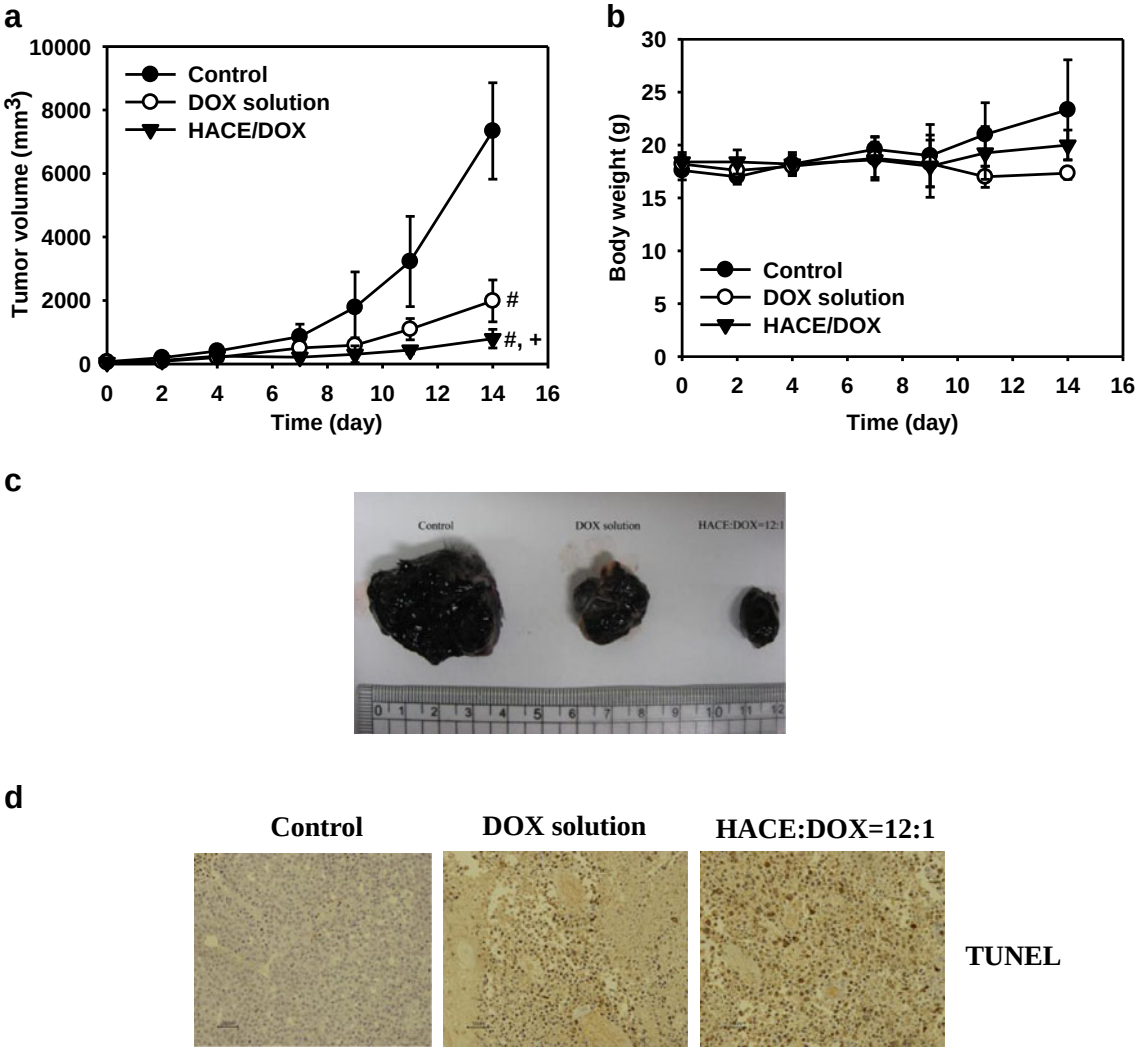

Fig. 7 *In vivo* antitumor efficacy test in the B16F10 tumor-bearing mouse model after intravenous injection. (**a**) The tumor size (mm^3) profile. DOX was intravenously injected at 4, 7, 9, and 11 days. $^{\#}P < 0.05$ compared with the control group; $^{+}P < 0.05$ compared with the DOX solution-treated group. (**b**) The body weight (g) profile. Each point represents the mean ± SD ($n \geq 4$). (**c**) Images of dissected tumors of all experimental groups after 14 days. (**d**) Microscopic images of the results of the TUNEL assay of dissected tumors after 14 days. The length of the bar is 50 μm.

results of a pharmacokinetic study previously (22). It can be concluded that the tumor targetability and lower clearance of DOX in the bloodstream could have resulted in the improved antitumor effect observed after the intravenous injection of HACE/DOX compared with DOX solution only.

In this investigation, the antitumor efficacy of the developed HACE-based NPs was also demonstrated after intratumoral injection. After intratumoral injection, it is thought that the DOX-loaded NP can be taken up into the cells through receptor-mediated endocytosis (HA-CD44 receptor interaction) and subsequently DOX exerted its antitumor efficacy after intercalating into the DNA backbone of the nucleus. Melanoma is known as a malignant cancer that occurs in easily accessible locations, such as the skin, eye, and respiratory epithelium, and can quickly spread to other tissues and organs (42). Intravenous injection as well as intratumoral injection of DOX-loaded NP was performed to identify its possible therapeutic efficacy for the metastasized melanoma nearby its primary site.

The results of the TUNEL assays of the dissected tumors are presented in Figs. 6d and 7d. The TUNEL assay has been used to detect the DNA fragmentation produced by apoptotic signaling cascades which is one of the principal anti-cancer mechanisms. In particular, the stronger brown staining observed in the HACE/DOX-treated groups administered through both injection groups revealed that apoptosis was significantly increased in the HACE/DOX NP-injected mice compared with that in mice in the other treatment groups. It appears likely that apoptosis may be one of the major

contributors toward the inhibition of tumor growth observed in this investigation.

CONCLUSIONS

DOX-loaded HACE-based NPs were prepared and their antitumor efficacy for melanoma was assessed. DOX-loaded NPs, characterized as having a mean diameter of approximately 110 nm, a narrow size distribution, and a high drug EE, were developed. *In vitro* DOX release was improved at an acidic pH compared with at a neutral pH. The cellular uptake of DOX seemed to be dependent on receptor-mediated endocytosis in B16F10 cells. Tumor growth was significantly inhibited in the B16F10 tumor-bearing mouse model after intratumoral and intravenous injection of the DOX-loaded NPs. Thus, it can be concluded that the HACE-based NPs developed in this study can be used as an effective anticancer drug delivery system for melanoma therapy.

ACKNOWLEDGMENTS AND DISCLOSURES

This work was supported by the National Research Foundation of Korea (NRF) grant funded by the Korean government (MEST) (No. 2011–0030635).

REFERENCES

1. Momparler RL, Karon M, Siegel SE, Avila F. Effect of adriamycin on DNA, RNA, and protein synthesis in cell-free systems and intact cells. Cancer Res. 1976;36(8):2891–5.
2. Laginha KM, Verwoert S, Charrois GJR, Allen TM. Determination of doxorubicin levels in whole tumor and tumor nuclei in murine breast cancer tumors. Clin Cancer Res. 2005;11(19):6944–9.
3. Von Hoff DD, Layard MW, Basa P, Davis HL, Von Hoff AL, Rozencweig M, *et al.* Risk factors for doxorubicin-induced congestive heart failure. Ann Intern Med. 1979;91(5):710–7.
4. Kawashima Y, Yamamoto H, Takeuchi H, Kuno Y. Mucoadhesive DL-lactide/glycolide copolymer nanospheres coated with chitosan to improve oral delivery of elcatonin. Pharm Dev Technol. 2000;5(1):77–85.
5. Choi KY, Chung H, Min KH, Yoon HY, Kim K, Park JH, *et al.* Self-assembled hyaluronic acid nanoparticles for active tumor targeting. Biomaterials. 2010;31(1):106–14.
6. Li N, Wang J, Yang X, Li L. Novel nanogels as drug delivery systems for poorly soluble anticancer drugs. Colloids Surf B Biointerfaces. 2011;83(2):237–44.
7. Chen MC, Tsai HW, Liu CT, Peng SF, Lai WY, Chen SJ, *et al.* A nanoscale drug-entrapment strategy for hydrogel-based systems for the delivery of poorly soluble drugs. Biomaterials. 2009;30(11):2102–11.
8. Mahmud A, Xiong X, Lavasanifar A. Development of novel polymeric micellar drug conjugates and nano-containers with hydrolyzable core structure for doxorubicin delivery. Eur J Pharm Biopharm. 2008;69(3):923–34.
9. Greish K. Enhanced permeability and retention of macromolecular drugs in solid tumors: A royal gate for targeted anticancer nanomedicines. J Drug Target. 2007;15(7–8):457–64.
10. Fukumori Y, Ichikawa H. Nanoparticles for cancer therapy and diagnosis. Adv Powder Technol. 2006;17(1):1–28.
11. Iinuma H, Maruyama K, Okinaga K, Sasaki K, Sekine T, Ishida O, *et al.* Intracellular targeting therapy of cisplatin-encapsulated transferrin-polyethylene glycol liposome on peritoneal dissemination of gastric cancer. Int J Cancer. 2002;99(1):130–7.
12. Kobayashi T, Ishida T, Okada Y, Ise S, Harashima H, Kiwada H. Effect of transferrin receptor-targeted liposomal doxorubicin in P-glycoprotein-mediated drug resistant tumor cells. Int J Pharm. 2007;329(1–2):94–102.
13. Dharap SS, Wang Y, Chandna P, Khandare JJ, Qiu B, Gunaseelan S, *et al.* Tumor-specific targeting of an anticancer drug delivery system by LHRH peptide. Proc Natl Acad Sci U S A. 2005;102(36):12962–7.
14. Laurent TC. The chemistry, biology and medical applications of hyaluronan and its derivatives. London: Portland; 1998.
15. Prestwich G, Marecak D, Marecek J, Vercruysse K, Ziebell M. Controlled chemical modification of hyaluronic acid: synthesis, applications, and biodegradation of hydrazide derivatives. J Control Release. 1998;53(1–3):93–103.
16. Price R, Berry M, Navsaria H. Hyaluronic acid: the scientific and clinical evidence. J Plastic Reconstr Aesthet Surg. 2007;60(10):1110–9.
17. Culty M, Shizari M, Thompson E, Underhill C. Binding and degradation of hyaluronan by human breast cancer cell lines expressing different forms of CD44: correlation with invasive potential. J Cell Physiol. 1994;160(2):275–86.
18. Akima K, Ito H, Iwata Y, Matsuo K, Watari N, Yanagi M, *et al.* Evaluation of antitumor activities of hyaluronate binding antitumor drugs: synthesis, characterization and antitumor activity. J Drug Target. 1996;4(1):1–8.
19. He M, Zhao Z, Yin L, Tang C, Yin C. Hyaluronic acid coated poly(butyl cyanoacrylate) nanoparticles as anticancer drug carriers. Int J Pharm. 2009;373(1–2):165–73.
20. Saddoughi SA, Song P, Ogretmen B. Roles of bioactive sphingolipids in cancer biology and therapeutics. In: Quinn PJ, Wang X, editors. Lipids in health and disease. Netherlands: Springer; 2008. p. 413–40.
21. Cho HJ, Yoon HY, Koo H, Ko SH, Shim JS, Lee JH, *et al.* Self-assembled nanoparticles based on hyaluronic acid-ceramide (HA-CE) and Pluronic® for tumor-targeted delivery of docetaxel. Biomaterials. 2011;32(29):7181–90.
22. Cho HJ, Yoon IS, Yoon HY, Koo H, Jin YJ, Ko SH, *et al.* Polyethylene glycol-conjugated hyaluronic acid-ceramide self-assembled nanoparticles for targeted delivery of doxorubicin. Biomaterials. 2012;33(4):1190–200.
23. Choi KY, Yoon HY, Kim JH, Bae SM, Park RW, Kang YM, *et al.* Smart nanocarrier based on PEGylated hyaluronic acid for cancer therapy. ACS Nano. 2011;5(11):8591–9.
24. Chang JE, Shim WS, Yang SG, Kwak EY, Chong S, Kim DD, *et al.* Liver cancer targeting of doxorubicin with reduced distribution to the heart using hematoporphyrin-modified albumin nanoparticles in rats. Pharm Res. 2012;29(3):795–805.
25. Cai S, Thati S, Bagby TR, Diab HM, Davies NM, Cohen MS, *et al.* Localized doxorubicin chemotherapy with a biopolymeric nanocarrier improves survival and reduces toxicity in xenografts of human breast cancer. J Control Release. 2010;146(2):212–8.
26. Luo Y, Bernshaw NJ, Lu ZR, Kopecek J, Prestwich GD. Targeted delivery of doxorubicin by HPMA copolymer-hyaluronan bioconjugates. Pharm Res. 2002;19(4):396–402.
27. Kim DH, An EJ, Kim J, Han SH, Kim JW, Oh SG, *et al.* Fabrication and characterization of pseudo-ceramide-based liposomal membranes. Colloids Surf B Biointerfaces. 2009;73(2):207–11.

28. Liao YH, Jones SA, Forbes B, Martin GP, Brown MB. Hyaluronan: pharmaceutical characterization and drug delivery. Drug Deliv. 2005;12(6):327–42.
29. Ma Y, Tang Y, Billingham NC, Armes SP, Lewis AL, Lloyd AW, *et al.* Well-defined biocompatible block copolymers via atom transfer radical polymerization of 2-methacryloyloxyethyl phosphorylcholine in protic media. Macromolecules. 2003;36(10):3475–84.
30. Lavasanifar A, Samuel J, Kwon GS. Micelles self-assembled from poly (ethylene oxide)-block-poly(N-hexyl stearate-aspartamide) by a solvent evaporation method: effect on the solubilization and haemolytic activity of amphotericin B. J Control Release. 2001;77(1–2):155–60.
31. Yokoyama M. Drug targeting with nano-sized carrier systems. J Artif Organs. 2005;8(2):77–84.
32. Liu D, Mori A, Huang L. Role of liposome size and RES blockade in controlling biodistribution and tumor uptake of GM1-containing liposomes. Biochim Biophys Acta. 1992;1104(1):95–101.
33. Gaucher G, Dufresne MH, Sant VP, Kang N, Maysinger D, Leroux JC. Block copolymer micelles: preparation, characterization and application in drug delivery. J Control Release. 2005;109 (1–3):169–88.
34. Choi YK, Lee DW, Yong CS, Choi HG, Bronich TK, Kim JO. Biostable poly(ethylene oxide)-*b*-poly(methacrylic acid) micelles for pH-triggered release of doxorubicin. J Pharm Invest. 2011;41(2):111–5.
35. Nukolova NV, Oberoi HS, Cohen SM, Kabanov AV, Bronich TK. Folate-decorated nanogels for targeted therapy of ovarian cancer. Biomaterials. 2011;32(23):5417–26.
36. Prabaharan M, Grailer JJ, Pilla S, Steeber DA, Gong S. Folate-conjugated amphiphilic hyperbranched block copolymers based on Boltorn® H40, poly(l-lactide) and poly(ethylene glycol) for tumor-targeted drug delivery. Biomaterials. 2009;30 (16):3009–19.
37. Liu H, Farrell S, Uhrich K. Drug release characteristics of unimolecular polymeric micelles. J Control Release. 2000;68 (2):167–74.
38. Fritze A, Hens F, Kimpfler A, Schubert R, Peschka-Süss R. Remote loading of doxorubicin into liposomes driven by a transmembrane phosphate gradient. Biochim Biophys Acta. 2006;1758(10):1633–40.
39. Eliaz RE, Nir S, Marty C, Szoka Jr FC. Determination and modeling of kinetics of cancer cell killing by doxorubicin and doxorubicin encapsulated in targeted liposomes. Cancer Res. 2004;64(2):711–8.
40. Kim EJ, Shim G, Kim K, Kwon IC, Oh YK, Shim CK. Hyaluronic acid complexed to biodegradable poly L-arginine for targeted delivery of siRNAs. J Gene Med. 2009;11(9):791–803.
41. Yang X, Grailer JJ, Rowland IJ, Javadi A, Hurley SA, Matson VZ, *et al.* Multifunctional stable and pH-responsive polymer vesicles formed by heterofunctional triblock copolymer for targeted anticancer drug delivery and ultrasensitive MR Imaging. ACS Nano. 2010;4(11):6805–17.
42. Godden D, Brennan PA, Milne J. Update on melanoma: the present position. Br J Oral Maxillofac Surg. 2010;48(8):575–8.